A plate-based assay system for analyses and screening of the *Leishmania major* inositol phosphorylceramide synthase

John G. Mina[1,2], Jackie A. Mosely[1], Hayder Z. Ali[1], Hosam Shams-Eldin[3], Ralph T. Schwarz[3,4], Patrick G. Steel[1,*] and Paul W. Denny[1,2,*]

[1]Biophysical Sciences Institute,

School of Biological and Biomedical Sciences and Department of Chemistry,

University Science Laboratories, South Road, Durham, DH1 3LE, UK

[2]School of Medicine and Health, Durham University,

Queen's Campus, Stockton-on-Tees, TS17 6BH, UK

[3]Institut für Virologie, Zentrum für Hygiene und Infektionsbiologie,

Philipps-Uniersität Marburg, Hans-Meerwein-Strasse, 35043 Marburg, Deutschland

[4]Unité de Glycobiologie Structurale et Fonctionnelle, UMR CNRS/USTL n° 8576 - IFR 118,

Université des Sciences et Technologies de Lille,

59655 Villeneuve D'Ascq cedex – France.

[*]Address correspondence to: Drs Paul W. Denny and Patrick G. Steel, Biophysical Sciences Institute, Department of Chemistry, University Science Laboratories, South Road, Durham, DH1 3LE, UK. http://www.bsi.dur.ac.uk Tel. +44 (0)191 334 3983 or +44 (0)191 334 2131; Email: p.w.denny@durham.ac.uk or p.g.steel@durham.ac.uk

Key words: Inositol phosphorylceramide synthase; *Leishmania* species; leishmaniasis; kinetics; inhibition

Abbreviations: PI – Phosphatidylinositol; PC – Phosphatidylcholine; IPC – Inositolphosphoryl ceramide; SM – Sphingomyelin; PSL – Phosphosphingolipid; NBD-C_6-ceramide – *N*-[6-[(7-nitro-2-1,3-benzoxadiazol-4-yl)amino]hexanoyl]-D-*erythro*-sphingosine; CHAPS – 3-[(3-cholamidopropyl) dimethylammonio]-1-propanesulfonate; *Lmj*IPCS – *Leishmania major* IPC synthase

Abstract

Sphingolipids are key components of eukaryotic membranes, particularly the plasma membrane. The biosynthetic pathway for the formation of these lipid species is largely conserved. However, in contrast to mammals, which produce sphingomyelin, organisms such as the pathogenic fungi and protozoa synthesize inositol phosphorylceramide (IPC) as the primary phosphosphingolipid. The key step involves the reaction of ceramide and phosphatidylinositol catalysed by IPC synthase, an essential enzyme with no mammalian equivalent encoded by the *AUR1* gene in yeast and recently identified functional orthologues in the pathogenic kinetoplastid protozoa. As such this enzyme represents a promising target for novel anti-fungal and anti-protozoal drugs. Given the paucity of effective treatments for kinetoplastid diseases such as leishmaniasis, there is a need to characterize the protozoan enzyme. To this end a fluorescent-based cell-free assay protocol in a 96-well plate format has been established for the *Leishmania major* IPC synthase. Using this system the kinetic parameters of the enzyme have been determined as obeying the double displacement model with apparent V_{max} = 2.31 pmol.min^{-1}.U^{-1}. Furthermore, inhibitory substrate analogues have been identified. Importantly this assay is amenable to development for use in high-throughput screening applications for lead inhibitors and as such may prove to be a pivotal tool in drug discovery.

1. Introduction

The insect vector borne protozoan parasites of the family Kinetoplastidae cause a range of human diseases, including the leishmaniases and African Sleeping Sickness. These infections are of increasing prevalence, particularly in developing countries, and have been classified by the World Health Organisation as Category I emerging or uncontrolled diseases (Remme, et al. 2002). For example, the *Leishmania* spp. (the causative agents of the leishmaniases) infect more than 12 million people in five continents and are endemic in 88 nation states putting over 350 million people at risk, with instances of leishmaniasis not uncommon in certain regions of North America and southern Europe. Moreover, the spread and severity of disease is exacerbated by its status as an important co-infection in AIDS patients and the overlap in prevalence of HIV and *Leishmania* (Alvar, et al. 2008). In the absence of effective vaccines, the treatment of kinetoplastid infections is difficult with the most serious visceral form of leishmaniasis often requiring a long, costly course of drug therapy. In addition, available drugs often exhibit serious side-effects and resistance is rapidly emerging (Remme, et al. 2002). These facts make the discovery and validation of new therapeutic agents a priority.

The diverse, amphipathic sphingolipids consist of a sphingoside backbone with long-chain base and polar alcohol attachments. These essential lipid species are found in all eukaryotic cells, as well as in some prokaryotic organisms and viruses (Smith and Merrill 2002). In eukaryotes, the unmodified sphingolipid, ceramide, is a precursor for the synthesis of complex sphingolipids in the Golgi apparatus. The resultant lipid species are subsequently concentrated in the outer leaflet of the plasma membrane. Here, together with sterols, they form the microdomains known as lipid rafts (Futerman and Hannun 2004). Such domains have been suggested to be central to a wide array of cellular processes, including the formation of signal transduction complexes (Magee, et al. 2002; Pierce 2002) and the polarized trafficking of lipid-modified proteins (Brown and London 1998). Importantly, sphingolipid metabolites such as ceramide and phosphorylated sphingosine (sphingosine-1-phosphate), are also involved in the intracellular signal transduction processes that regulate cell growth, differentiation and programmed cell death (apoptosis) (Futerman and Hannun 2004).

Sphingolipids demonstrate structural divergence in evolution. Whilst sphingomyelin (SM) is the predominant phosphosphingolipid (PSL) of mammalian cells, inositol phosphorylceramide (IPC) is found in the fungi, plants and some protozoa but not in

mammals (Lester and Dickson 1993; Sperling and Heinz 2003). SM is formed by the transfer of the phosphorylcholine head group from the phospholipid phosphatidylcholine (PC) to ceramide, a reaction catalyzed by SM synthase (Huitema, et al. 2004). The related enzyme, IPC synthase, mediates the formation of IPC in fungi, plants and the pathogenic kinetoplastid protozoa (e.g. *Leishmania* spp.) by catalyzing the transfer of phosphorylinositol from phosphatidylinositol (PI) to ceramide or phytoceramide (Becker and Lester 1980; Bromley, et al. 2003; Denny, et al. 2006). In the fungi this enzyme activity has been attributed to the AUR1p protein first identified in *Saccharomyces cerevisiae* and subsequently in several fungal pathogens (Heidler and Radding 1995; Heidler and Radding 2000). We have isolated a functional orthologue of this protein in the kinetoplastid, protozoan parasite *Leishmania major* (*Lmj*IPCS) (Denny, et al. 2006). *Lmj*IPCS is encoded by a single gene (GeneDB, *Lmj*F35.4990), and closely related orthologues are found in the complete genome sequences of the related kinetoplastid pathogens, *Trypanosoma brucei* (the causative agent of African Sleeping Sickness) and *T. cruzi* (Chagas Disease) (Denny, et al. 2006). IPC synthase activity is evident in both the insect and mammalian stages of the *L. major* lifecycle, however in the intra-macrophage form the parasite is predicted to scavenge host cell ceramide for use as substrate by *Lmj*IPCS (Zhang, et al. 2005; Zhang, et al. 2009).

As an essential activity with no mammalian equivalent the fungal IPC synthase has become a recognized and well studied drug target (Georgopapadakou 2000; Nagiec, et al. 1997). The discovery of functional orthologues in the kinetoplastid pathogenic protozoa has led to its further consideration as an anti-protozoal target (Suzuki, et al. 2008). It is known that *Lmj*IPCS activity is susceptible to the established fungal inhibitor aureobasidin A (Denny, et al. 2006). In addition, this compound has been demonstrated to inhibit the growth and infectivity of *L. amazonensis* (Tanaka, et al. 2007). Furthermore, recent work in our laboratory (Mina, et al. 2009) and elsewhere (Sutterwala, et al. 2008) has both genetically and pharmacologically validated the kinetoplastid enzyme as a target in *T. brucei*. Therefore, further study of the *Lmj*IPCS (and other kinetoplastid orthologues) is vital in moving towards the ultimate goal of identifying compounds with the potential for development into much needed, pharmacologically active anti-protozoals. Herein we report the establishment of a robust 96-well plate based assay system that uses easily obtainable, transgenic yeast-derived material, together with its application to detail the kinetic parameters of *Lmj*IPCS and demonstrate the inhibitory effects of several substrate analogues.

2. Materials and Methods

2.1. Materials

Phosphatidylinositol (bovine liver PI; predominant species 1-stearoyl-2-arachidonoyl-*sn*-glycero-3-phospho-1'-myo-inositol sodium salt) was from Avanti Polar Lipids. D-*erythro*-sphingosine (d18:1; sphing-4-enine, (2*S*,3*R*,*E*)-2-aminooctadec-4-ene-1,3-diol) and N-acetyl-D-*erythro* sphingosine (d18:1/2:0; *N*-acetyl-sphing-4-enine, (2*S*,3*R*,4*E*)-*N*-acetyl-2-aminooctadec-4-ene-1,3-diol) were from TOCRIS BioScience. C_{18}-Ceramide (d18:1/18:0; *N*-stearoyl-D-*erythro*-sphingosine, (2*S*,3*R*,4*E*) *N*-stearoyl-2-aminooctadec-4-ene-1,3-diol) and diacylglycerol (1-octadecanoyl-2-(5Z,8Z,11Z,14Z-eicosatetraenoyl)-*sn*-glycerol) were from Sigma Aldrich. NBD-C_6-ceramide (*N*-[6-[(7-nitro-2-1,3-benzoxadiazol-4-yl)amino]hexanoyl]-D-*erythro*-sphingosine) was from Invitrogen.

2.2. Preparation of *Lmj*IPCS microsomal material

Auxotrophic AUR1 mutant *Saccharomyces cerevisiae* was complemented by the expression of the *L. major* IPC synthase to create YPH499–HIS–GAL–AUR1 pRS246 *Lmj*IPCS (Denny, et al. 2006). These cells were propagated in SD medium (0.17% Bacto yeast nitrogen base, 0.5% ammonium sulphate and 2% dextrose) containing the appropriate nutritional supplements, and microsomes prepared from an exponentially growing culture (Fischl et al., 2000). Briefly, approximately 8.0 g of wet cell mass was suspended in STE buffer (25 mM Tris HCl pH 7.4, 250 mM sucrose and 1 mM EDTA) containing Complete® EDTA-free Protease Inhibitor Cocktail (Roche Applied Science) and the yeast disrupted by vortex mixing with pre-chilled acid-washed glass beads (425-600 *μ*m, Sigma Aldrich). After the removal of the glass beads, unbroken cells and cell-wall debris by centrifugation (1500g, 4°C and 15 minutes), the microsomal membrane fraction was isolated by differential centrifugation. Subsequently the large granular fraction was removed (27000 g, 4 °C and 30 minutes) and the microsomal membrane fraction isolated (150000 g, 4 °C and 90 minutes). The microsomes were re-suspended at a concentration of 10 mg.ml^{-1} in storage buffer (50 mM Tris/HCl pH 7.4, 20% (v/v) glycerol, 5 mM $MgCl_2$) containing protease inhibitor. As required, the microsomal membranes were washed in 2.5% CHAPS (Sigma Aldrich; 4 °C, 60 minutes), isolated by centrifugation (150000 g, 4°C and 90 minutes), assayed for protein content (CBQCA, Invitrogen) and re-suspended in storage buffer. A second wash inactivated the enzyme.

Different preparations of microsomal membranes were utilized in this study and these varied in specific *Lmj*IPCS enzyme activity. Therefore, to standardise the assay material

samples were normalized with respect to active enzyme content ensuring consistency across experiments. Although the standardised unit for enzymatic activity is the katal where 1 kat = 1 mol(product).s^{-1} (International Union of Biochemistry, 1979), for the range of substrates concentrations used in the work presented here a more practical value is enzyme unit (U). One unit (U) of enzyme is defined as that which converts 1 pmol of substrate per minute under the conditions described (1 U = 1 pmol(product).min^{-1}), where 1 U corresponds to 16.67 *femto*kats (Fischl et al., 2000)**.** The conversion of the fluorescent acceptor substrate NBD-C$_6$-ceramide to the product NBD-C$_6$-IPC was measured and quantified with respect to known concentrations of NBD-C$_6$-ceramide, activity calculated as U.μl^{-1} and the samples were stored at -80 °C until use. Enzyme turnover was calculated per milligrams of total protein in the sample (U.mg^{-1}).

2.3. Thin layer chromatography (TLC) based *Lmj*IPCS synthase assay

Both unwashed and CHAPS-washed (1 μg) microsomal membranes were used in a 50 μl assay mix containing 1 mM PI, 100 mM Tris HCl (pH7.4) and 200 μM NBD-C$_6$-ceramide (Figueiredo et al., 2005). The reaction was pre-incubated before the addition of the NBD-C$_6$-ceramide at 30 °C (the established optimum temperature in the assay) for 30 minutes and subsequently for a further hour before quenching with 150 μl of chloroform:methanol:water (10:10:3). After biphasic separation the organic layer was removed, dried in a rotavapor (Eppendorf Concentrator 5301) and re-suspended in 20 μl of 10:10:3. The reaction products were fractionated using HPTLC silica plates (Merck) and the eluent system chloroform:methanol:aqueous 0.25% KCl (55:45:10). The R_f values for the substrate, NBD-C$_6$-ceramide, and the product, NBD-C$_6$-IPC were 0.96 and 0.57 respectively. Quantification was carried out using a FLA3000 scanner (Fujifilm) and AIDA Image Analyzer$^\circledR$ software (version 3.52).

2.4. 96-well plate-based LmjIPCS synthase assay for kinetic analyses

CHAPS-washed membranes (Aeed, et al. 2004), 0.6 U or as described, were used in a reaction mix containing 100 μM (or as indicated) PI, 50 mM KH$_2$PO$_4$ (pH7.0) and 5 μM (or as indicated) NBD-C$_6$-ceramide. Following pre-incubation at 30°C for 30 minutes, the reaction was initiated by the addition of the NBD-C$_6$-ceramide (5 μM or as indicated) and 2.4 mM CHAPS. The reaction was incubated for the specified period of time and subsequently quenched by the addition of 200 μl of methanol. Separation of the reaction product, NBD-C$_6$-IPC, from the substrate NBD-C$_6$-ceramide was achieved by applying the

reaction mix to 100 μl (sedimented gel volume) of AG4-X4 resin (BioRad), formate form, in 96-well Multiscreen® Solvinert filter plates (Millipore) using a vacuum manifold (Millipore). The resin was washed 5 times with 200 µl methanol, the product was eluted into OptiPlate™ 96-F plates (Perkin Elmer) using 200 µl of 1 M potassium formate in methanol and quantified using a fluorescence plate reader (FLx800™, BioTek) - excitation λ = 485 nm; emission λ = 528 nm. Assays used were carried out in triplicate and results analysed using Prism 5.0 software (GraphPad) and Excel® Solver Add-in (Microsoft Office). The separation protocol was validated by collecting fractions from a 5-fold scale up of the process and fractionating them by TLC as above (figure 1).

Substrate analogues were employed in inhibition studies and added with the fluorescent substrate NBD-C_6-ceramide in the quantities indicated.

The assay system was validated as excellent for screening purposes with a Z' value of 0.58 (Zhang, et al. 1999). Calculation of this value utilized 2 bespoke inhibitors, (*4E*) *N-(phenylacetyl)-1-deoxy-sphing-4-enine* and (*2R,4E*) *N-phenylacetyl2-aminooctadec-4-en-1-ol* whose synthesis and screening will be subsequently reported.

2.5. Mass spectrometry

Analyses were performed on an LTQFT (ThermoFinnigan Corp); an FTICR MS instrument equipped with a 7.0 T magnet. Chloroform extracts were introduced into the electrospray ion source by direct infusion from a syringe at a flow rate of 3 μl.min^{-1}. Positive ion measurements were made with the source voltage at 4.0 kV and negative ion measurements were made with the source voltage at 3.5 kV. The tube lens was kept at 100 V and the source temperature at 275 °C for all experiments.

2.6. Cytotoxicity screening

L. major (MHOM/IL/81/Friedlin) and *L. mexicana* (MNYC/BZ/62/M379) parasites were maintained at 26 °C in Schneider's Drosophila media (Sigma Aldrich) supplemented with heat inactivated foetal bovine sera (15% for promastigotes and 20% for amastigotes; Biosera). *L. mexicana* promastigotes were transformed into axenic amastigotes by a pH and temperature shift as previously described (Bates, 1994). In 96-well plates (Nunc) parasites at 10^5ml^{-1} were incubated with compounds in triplicate (including miltefosine (Cayman Chemical) as a positive control, and untreated parasites and media as negative controls) for 24 hours before incubation with Alamar Blue (Invitrogen) for 4 hours prior to assessing cell viability using a fluorescent plate reader (Biotek; 560EX nm/600EM nm).

LD₅₀ was calculated after plotting cell viability (as % of untreated control) against log compound concentration (*µ*M).

3. Results and Discussion

3.1. Assay of *Lmj*IPCS microsomal material

The high levels of endogenous PI present in yeast microsomes (Aeed, et al. 2004) rendered establishing the kinetic parameters of *Lmj*IPCS with respect to this donor substrate problematic. Initial assay experiments using unrefined material derived from *Lmj*IPCS complemented HIS-GAL-AUR1 auxotrophic yeast IPCS mutants (Denny, et al. 2006) demonstrated that endogenous, microsomal PI accounted for approximately 25% of the measured *Lmj*IPCS turnover (figure 2A), making accurate determination of the enzyme kinetic parameters impossible. A similar problem has previously been identified with the use of *Trypanosoma cruzi* derived microsomes in an assay of *Tc*IPCS turnover (Figueiredo, et al. 2005). However, it has been demonstrated that washing microsomal membranes derived from the pathogenic yeast, *Candida albicans* with a zwitterionic detergent (CHAPS) removed endogenous substrate lipids without affecting IPCS activity (Aeed, et al. 2004). Adopting this approach and employing microsomes from *Lmj*IPCS complemented HIS-GAL-AUR1 yeast, washed with CHAPS as described, the parasite enzyme assay proved to be dependent not only on the addition of the fluorescent acceptor substrate, NBD-C_6-ceramide, but now also more than 90% dependent on the addition of the donor substrate (bovine liver PI; figure 2A). It has previously been demonstrated that the *S. cerevisiae* orthologous enzyme, AUR1p, is unable to utilise bovine liver PI (Mina, et al. 2009). In the present assay system, the CHAPS-washed microsomes also demonstrated an approximately 2-fold higher level of enzyme turnover than equivalent quantities of crude material (figure 2B). This increase is most likely due to enrichment of the sample for *Lmj*IPCS as other proteins are washed away from the detergent insoluble material. However, the removal of microsomal proteins and lipids may also reduce the spatial volume of the washed material leading to more rapid diffusion of applied exogenous substrates into the membranes. Taken together these data indicate that washing the microsomes with CHAPS depletes them of PI, and perhaps (phyto)ceramide, thereby facilitating more accurate determination of the kinetics of *Lmj*IPCS. Moreover, the fact that *Lmj*IPCS remained highly active within a detergent resistant lipid environment suggests that the enzyme may reside within CHAPS-resistant lipid microdomains *in vivo* (Rouvinski, et al. 2003).

3.2. Determination of *Lmj*IPCS assay parameters

Using the 96-well plate formatted system described, reproducible, quantitative kinetic data could be obtained for the enzyme from CHAPS-washed *Lmj*IPCS yeast microsomes. In the first instance the formation of product (IPC) over time was determined. The results demonstrated that the reaction rate is linear for 30 minutes before it decreases over time (figure 3A). As a consequence all subsequent assays were performed with a 15 minute reaction time to ensure linearity under the specified conditions, turnover was assumed to be equivalent to initial velocity (v_0).

Since both substrates are in excess and only approximately 12 % of the limiting acceptor substrate, NBD-C_6-ceramide, is consumed after 1 hour, the reasons for the decrease in reaction rate above 30 minutes are unclear. The IPC product may be localised around the enzyme affecting a change in the diffusion rate of the substrates to the active site. It is also possible that *Lmj*IPCS activity is modulated by inhibitory feedback from the synthesized NBD-C_6-IPC or diacylglycerol (DAG) which is formed as a by-product of IPC synthase turnover (Denny, et al. 2006). Analysis of the inhibitory affect of DAG indicated a logIC_{50} value of 0.92±0.8 and an IC_{50} of 8.3 µM (figure 3B) supporting the latter hypothesis.

Product (NBD-C_6-IPC) formation also increased in a linear manner with increasing enzyme concentration up to 0.8 U/assay (figure 3C). However, the linear relationship deviated beyond this point (data not shown). Notably, increasing the concentration of enzyme also leads to a change in the protein : lipid : detergent (CHAPS) ratio and hence modulates the substrate concentration at the active site of *Lm*IPCS. Taking this observation into account 0.6 U of *Lm*IPCS (within the linear range) was employed in all subsequent analyses.

3.3 Determination of *Lmj*IPCS kinetic parameters

Having established a standardized set of conditions that gave a linear response, and in which endogenous interfering substrate was minimized by detergent washing, the kinetic parameters of *Lmj*IPCS with respect to both the acceptor (NBD-C_6-ceramide) and donor (PI) substrates were determined. Initially, the data obtained were tested against the Michaelis-Menten model and with respect to increasing concentrations of NBD-C_6-ceramide gave a curve of good fit (R^2 = 0.97; figure 4A). The apparent K_m for the acceptor substrate was 3.5±0.35 μM and the apparent V_{max} 2.1±0.07 pmol.min^{-1}.U^{-1}. However, determination of the Hill constant revealed a Hill slope of 2.7 that indicated co-operative binding of substrates was occurring (Hill 1910).

In contrast, with [NBD-C_6-ceramide] fixed at 5 µM, the data with respect to the PI showed a poor fit to the Michaelis-Menten equation (R^2 = 0.82; figure 4B), with considerable deviation at high concentrations of donor substrate. The enzyme orthologue from the pathogenic yeast *C. albicans* has previously been shown to behave in a similar manner, a phenomenon which was described as being caused by substrate inhibition (Aeed, et al. 2004). However, at a higher, saturating concentration of the acceptor substrate, [NBD-C_6-ceramide] = 20 µM (> 5x apparent K_m), no apparent inhibition at high [PI] could be detected (figure 4C). This strongly suggested that activity is dependent on the substrate molar ratio, with a dilution effect being observed with low NBD-C_6-ceramide (5 µM) and high PI (>150 µM). The % molar concentration of NBD-C_6-ceramide dropped 30% from 0.82% at 12.5 µM PI and 600 µM CHAPS to 0.58% 250 µM PI and 600 µM CHAPS. In contrast a change in concentration of the acceptor substrate has little affect on the % molar concentration of PI (14.3% at 1 µM NBD-C_6-ceramide and 600 µM CHAPS to 13.9% 20 µM NBD-C_6-ceramide NBD-C_6-ceramide and 600 µM CHAPS) and CHAPS concentration.

PI vesicles can be solubilised by CHAPS far below the CMC of this detergent at 0.27 mM ($[D_w]^c$: critical concentration of free detergent; Schürholz 1996). Therefore under the experimental conditions employed (0.6mM CHAPS) in the assay system PI/CHAPS mixed micelles are formed. The molar detergent to lipid ration of these micelles (R^c) is 0.17, meaning that CHAPS is a minor component, approximately 15% of the total molar concentration in micelles (Schürholz 1996). Based on these data the $[D_w]^c$ in the assay system employed can be calculated using Equation 1 (Schürholz 1996).

$$[D_T]^C = [D_w]^C + R^C(M) \times [L_T]$$

$[D_T]^C$ = Total CHAPS concentration,   **Equation 1**

$[L_T]$ = Total lipid concentration

At $[D_T]^c$= 600 μM in the reaction mix the $[D_w]^c$ (270μM) is exceeded under all conditions employed in this study and CHAPS exists primarily in a monomeric form with a minor proportion associated with PI in micelles (2.8% at 100μM PI).

Given the fact in this complex system the *Lmj*IPCS is a membrane enzyme acting on lipid substrates within mixed micelles the deviation from Michaelis-Mention kinetics observed is unsurprising. To facilitate further analyses a number of assumptions were made, namely: the kinetic parameters would be determined using the steady state approach; initial rate assumptions are applied; PI/CHAPS micelles have a low molar % of CHAPS (approximately 15%); all lipids and detergent molecules have the same surface area; all lipids and detergent molecules have equal accessibility to the enzyme active site. All concentrations are expressed as molar fractions of total lipid plus detergent

Subsequently a series of assay reactions were carried out with varying acceptor substrate concentrations, [NBD-C_6-ceramide], at different fixed [PI] (12.5 − 100 μM). A global analysis of the data points (56 mean points of 168 replicates) employing the surface dilution kinetic model, which considers the surface concentration of lipids ([PI] and [Cer] expressed as mol% in PI/CHAPS micelles; Deems, et al. 1975), resulted in non-convergent results. However, given that *Lmj*IPCS is an integral membrane protein within microsomal membranes the enzyme can fuse with PI/CHAPS micelles, or maintain its integrity and bounce between micelles whilst interacting with the bulk monomeric CHAPS/NBD-C_6-ceramide in the assay buffer. Both cases would confer bulk concentration dependence to the kinetics (Carman, et al. 1995).

Lineweaver-Burk analyses of the data set gave a near parallel pattern (figure 5A), with a plot of the intercepts demonstrating a linear correlation to 1 / [PI] molar % (figure 5B). A subsequent global analysis of these data in terms of a generalised form of a bi-bi substrate kinetic equation (Engel 1977; Equation 2) provided a solution for the values of the equation parameters, where $\emptyset_0$ = 0.26, $\emptyset_A$ = 0.82, $\emptyset_B$ = 0.14, $\emptyset_{AB}$ = 1.0 × 10^{-5}. From these V_{max} = 2.31 pmol.min^{-1}.min^{-1}, K_m [PI] = 3.15 molar % and K_m [NBD-C_6-ceramide] = 0.54 molar %.

$$\frac{[E_T]}{v} = \varnothing_0 + \varnothing_A \frac{1}{[\text{PI}]} + \varnothing_B \frac{1}{[\text{Cer}]} + \varnothing_{AB} \frac{1}{[\text{PI}][\text{Cer}]} \qquad \textbf{Equation 2}$$

Notably, the relatively high affinity of the acceptor substrate for *Lmj*IPCS compared with that of the donor PI was consistent with the proposal that ceramide, a highly bioactive molecule, is the rate-limiting substrate in the *in situ* IPC synthase reaction. In contrast PI is a relatively abundant substrate in most membraneous environments (Aeed, et al. 2004; Dickson 1998; Leber, et al. 1995).

Based on these data the value $\varnothing_{AB}$ was assumed to be zero thereby reducing Equation 2 to that describing double displacement kinetics (Equation 3). Details of the factors of $\varnothing_0$, $\varnothing_A$, $\varnothing_B$ is detailed in supplementary data (S1).

$$\frac{[E_T]}{v} = \varnothing_0 + \varnothing_A \frac{1}{[\text{PI}]} + \varnothing_B \frac{1}{[\text{Cer}]} \qquad \textbf{Equation 3}$$

These analyses provide strong support for the notion that *Lmj*IPCS functions via a double displacement model. This is further evidenced by the close correlation of experimental data with simulations derived from Equation 3 (figure 5C and D).

With this in mind, the apparent fit to the Michaelis-Menton model with respect to ceramide initially observed was most likely due to pre-incubation with saturating levels of PI leaving the majority of the enzyme in an intermediate phosphorylated state. In this state it is predicted that *Lmj*IPCS has mediated the transfer of the phosphorylinositol group of PI to the reactive histidine within the identified catalytic triad (Denny, et al. 2006) with the concomitant release of DAG. Notably mutation of His-294 within the yeast AUR1p triad has been shown to result in non-viable haploid cells (Levine, et al. 2000) and the equivalent mutation (His-264) in *Lmj*IPCS rendered it unable to complement auxotrophic AUR1p mutant yeast (Mina and Denny, unpublished). The second step in the reaction is then initiated by the addition of acceptor substrate (ceramide) when the phosphorylated intermediate is subjected to nucleophilic attack by the oxygen of the ceramide hydroxyl group, resulting in phosphoryl group transfer to the sphingoid base thus forming IPC.

3.4. Substrate analogues as competitive inhibitors

The delineation of the kinetic parameters of LmjIPCS also provided the opportunity to begin to further understand the mode of action of this enzyme and perhaps, via a rational approach, to design specific inhibitors. Given the high affinity of the acceptor substrate for LmjIPCS, the ability of natural ceramide (Cer; 18:1/18:0; N-stearoyl-D-*erythro*-sphingosine) and the ceramide analogues D-*erythro*-sphingosine and N-acetyl-D-*erythro*-sphingosine to compete with fluorescent NBD-C_6-ceramide was analyzed, with variation in the quantity of the product (NBD-C_6-IPC) reflecting the effect of the substrate competitors on enzyme turnover.

Unlike N-acetyl-D-*erythro*-sphingosine and D-*erythro*-sphingosine, N-stearoyl-D-*erythro*-sphingosine was insufficiently soluble in the phosphate-based buffer employed for the microtitre plate assay, curtailing analysis. This problem could be circumvented by using a Tris-based buffer system containing defatted-BSA. Here N-stearoyl-D-*erythro*-sphingosine was soluble and the results indicated that NBD-C_6-ceramide exhibited an affinity for LmjIPCS equivalent to that of the natural substrate (data not shown). Analyses of the more soluble synthetic analogues, N-acetyl-D-*erythro*-sphingosine and D-*erythro*-sphingosine, using the phosphate-based buffer system in the 96-well plate based assay demonstrated that they are, as expected, competitive with respect to NBD-C_6-ceramide: IC_{50} values of 16 µM and 52 µM respectively (figure 6A and B). Subsequent MS-ES$^+$/ES$^-$ analyses of the reaction product profiles (figure 7) revealed the presence of a mass of 582.3 corresponding to IP-N-acetyl-D-*erythro*-sphingosine confirming that N-acetyl-D-*erythro*-sphingosine had been turned over by LmjIPCS. This was expected as this ceramide analogue has previously been shown to act as a substrate for the yeast enzyme (Nagiec, et al. 1997). Conversely, no IP-D-*erythro*-sphingosine could be detected in the MS spectra either in positive or negative ion mode, which indicated that D-*erythro*-sphingosine is not a substrate for LmjIPCS, rather it is acting as a true inhibitor (data not shown). Screening this inhibitor against *L. major* and *L. mexicana* promastigotes (insect stage) and *L. mexicana* amastigotes (mammalian stage) demonstrated its efficacy against both species and lifecycle stages (LD_{50} of 6.5µM, 8.2 µM and 13.3µM respectively; table 1). It should be noted that it is unclear whether this was a target specific effect, however the substrate analogue N-acetyl-sphingosine was considerably less cytotoxic such that it was not possible to determine its LD_{50} versus *L. mexicana* amastigotes (table 1).

In structure-function terms these data indicated that the free-amino group present in D-*erythro*-sphingosine abolishes enzyme activity, whilst masking this group with even a minimal acyl moiety (*N*-acetyl-D-*erythro*-sphingosine) restored it. Similarly, sphingosine analogues have demonstrated an inhibitory effort on the *S. cerevisiae* phosphatidate phosphatase (Wu, et al. 1993)*,* a member of the LPP enzyme superfamily which are believed to share a mechanism of action with the sphingolipid synthases (Huitema, et al. 2004). Taken together it may be hypothesized that the protonated free-amino group of D-*erythro*-sphingosine electrostatically interferes with the active site of these enzymes, an observation which may potentially be exploited in the rational design of specific enzyme inhibitors.

4. Summary

Using the multi-well format assay established in this work we have deduced the kinetic parameters of *Lmj*IPCS with respect to both the donor (PI) and acceptor (NBD-C$_6$-ceramide) substrates, and provided evidence that the enzyme functions through a bi-bi (ping-pong) substrate kinetic model. These data provide the first direct indication of the mechanism of action of the sphingolipid synthase family. Such analyses would not have been possible using a conventional assay system such as that previously employed for the *T. cruzi* orthologue (Figueiredo, et al. 2005). However, by employing a complemented yeast system, large quantities of active *Lmj*IPCS could be isolated in a cost effective manner avoiding the handling of pathogenic material. Furthermore washing the microsomal starting material with CHAPS removed endogenous, contaminating donor substrate (PI) leaving an environment in which the enzyme exhibited not only a dependency on exogenous PI, but also a higher level of specific activity.

With a *Z'* value of 0.58 (Zhang, et al. 1999), the assay system described lends itself to high-throughput screening for inhibitors of a protozoal enzyme activity that has been demonstrated to be essential for kinetoplastid pathogens (Mina, et al. 2009; Sutterwala, et al. 2008). The assay of ceramide analogues demonstrated this potential and provides the backbone for consideration of rationally designed enzyme inhibitors. In the longer term, it is hoped that it will assist in the discovery of new, much needed therapies for leishmaniasis and African sleeping sickness.

15

Acknowledgements

References

Aeed PA, Sperry AE, Young CL, Nagiec MM, Elhammer ÅP. Effect of membrane perturbants on the activity and phase distribution of inositol phosphorylceramide synthase, development of a novel assay. Biochemistry 2004;43:8483 - 93

Alvar J, Aparicio P, Aseffa A, Den Boer M, Cañavate C, Dedet JP, Gradoni L, Ter Horst R, López-Vélez R, Moreno J. The relationship between leishmaniasis and AIDS: the second 10 years. Clin Microbiol Rev 2008;21:334 -359

Bates, PA. Complete developmental cycle of *Leishmania mexicana* in axenic culture. Parasitol 1994;108: 1-9

Becker GW, Lester RL. Biosynthesis of phosphoinositol-containing sphingolipids from phosphatidylinositol by a membrane preparation from *Saccharomyces cerevisiae*. J Bacteriol 1980;142:747 - 54

Bromley PE, Li YO, Murphy SM, Sumner CM, Lynch DV. Complex sphingolipid synthesis in plants: characterization of inositolphosphorylceramide synthase activity in bean microsomes. Arch Biochem Biophys 2003;417:219 - 26

Brown DA, London E. Functions of lipid rafts in biological membranes. Annu Rev Cell Dev Biol 1998;14:111 - 36

Carman GM, Deems RA, Dennis EA. Lipid signaling enzymes and surface dilution kinetics. J Biol Chem 1995;270:18711 - 14

Demms RA, Eaton BR, Dennis EA. Kinetic anlaysis of phospholipase A-2 activity toward mixed micelles and its implications for the study of liplytic enzymes. J Biol Chem 1975;250:9013 - 20

Denny PW, Shams-Eldin H, Price HP, Smith DF, Schwarz RT. The protozoan inositol phosphorylceramide synthase: a novel drug target which defines a new class of sphingolipid synthase J Biol Chem 2006;281:28200- 09

Dickson RC. Sphingolipid functions in *Saccharomyces cerevisiae*: comparision to mammals. Annu Rev Biochem 1998;67:27 - 48

Engel CP. Enzyme kinetics: The steady-state approach 1 st ed. John Wiley & Sons; 1977

Figueiredo JM, Dias WB, Mendonca-Previato L, Previato J, Heise N. Characterization of the inositol phosphorylceramide synthase activity from *Trypanosoma cruzi*. Biochem J 2005;387:519 - 29

Fischl AS, Liu Y, Browdy A, Cremesti AE. Inositolphosphorylceramide synthase from yeast. Methods Enzymol 2000;311:123 - 130

Futerman AH, Hannun YA. The complex life of simple sphingolipids. EMBO Reports 2004;5:777 - 82

Georgopapadakou NH. Antifungals targeted to sphingolipid synthesis: focus on inositol phosphorylceramide synthase. Expert Opin Investig Drugs 2000;9:1787 - 96

Heidler SA, Radding JA. The AUR1 gene in *Saccharomyces cerevisiae* encodes dominant resistance to the antifungal agent aureobasidin A (LY295337). Antimicrob Agents Chemother 1995;39:2765 - 69

Heidler SA, Radding JA. Inositol phosphoryl transferases from human pathogenic fungi. Biochim Biophys Acta 2000;1500:147 - 52

Hill AV. The possible effects of the aggregation of the molecules of huemoglobin on its dissociation curves. Proc Physiol Soc 1910 40(suppl):4 - 7

Huitema K, van den Dikkenberg J, Brouwers JF, Holthuis JC. Identification of a family of animal sphingomyelin synthases. Embo J 2004;23:33 - 44

International Union of Biochemistry. Units of enzyme activity. Eur J Biochem 1979;97:319 - 20

Leber A, Hrastnik C, Daum G. Phospholipid-synthesizing enzymes in Golgi membranes of the yeast, *Saccharomyces cerevisiae*. FEBS Lett 1995;377:271 - 274

Lester RL, Dickson RC. Sphingolipids with inositolphosphate-containing head groups. Adv Lipid Res 1993;26: 253 - 74

Levine TP, Wiggins CA, Munro S. Inositol phosphorylceramide synthase is located in the Golgi apparatus of *Saccharomyces cerevisiae*. Mol Biol Cell 2000;11:2267 - 81

Magee T, Prinen N, Alder J, Pagakis SN, Parmryd I. Lipid rafts: cell surface platforms for T-cell signalling. Biol Res 2002;35:127 - 31

Mina JG, Pan SY, Wansadhipathi NK, Bruce CR, Shams-Eldin H, Schwarz RT, Steel PG, Denny PW. The *Trypanosoma brucei* sphingolipid synthase, an essential enzyme and drug target. Mol Biochem Parasitol 2009;1688:16 - 23

Nagiec MM, Nagiec EE, Baltisberger JA, Wells GB, Lester RL, Dickson RC. Sphingolipid synthesis as a target for antifungal drugs. J Biol Chem 1997;272:9809 - 17

Nagiec MM, Nagiec EE, Baltisberger JA, Wells GB, Lester RL, Dickson RC. Sphingolipid synthesis as a target for antifungal drugs. Complementation of the inositol phosphorylceramide synthase defect in a mutant strain of *Saccharomyces cerevisiae* by the AUR1 gene. J Biol Chem 1997;272:9809 - 17

Pierce SK. Lipid rafts and B-cell activation. Nature Rev Immunol 2002;2:96 - 105

Remme JHF, Blas E, Chitsulo L, Desjeux PMP, Engers HD, Kanyok TP, Kengeya Kayondo JF, Kioy DW, Kumaraswami V, Lazdins JK, Nunn PP, Oduola A, Ridley R, Toure Y, Zicker F, Morel CMM. Strategic emphases for tropical diseases research: a TDR perspective. Trends Parasitol 2002;18:421 - 26

Rouvinski A, Gahali-Sass I, Stav I, Metzer E, Atlan H, Taraboulos A. Both raft- and non-raft proteins associate with CHAPS-insoluble complexes: some APP in large complexes. Biochem Biophys Res Commun 2003;308:750 - 58

Schürholz T. Critical dependence of the solubilization of lipid vesicles by the detergent CHAPS on the lipid composition. Functional reconstitution of the nicotinic acetylcholine receptor into preformed vesicles above the critical micellization concentration. Biophysical Chemistry 1996;58:87 - 96

Smith WL, Merrill AH. Sphingolipid metabolism and signaling. J Biol Chem 2002;277:25841 - 42

Sperling P, Heinz E. Plant sphingolipids: structural diversity, biosynthesis, first genes and functions. Biochim Biophys Acta 2003;1632:1 - 15

Sutterwala SS, Hsu FF, Sevova ES, Schwartz KJ, Zhang K, Key P, Turk J, Beverley SM, Bangs JD. Developmentally regulated sphingolipid synthesisin African trypanosomes. Mol Microbiol 2008;70:281 - 96

Suzuki E, Tanaka AK, Toledo MS, Levery SB, Straus AH, Takahashi HK. Trypanosomatid and fungal glycolipids and sphingolipids as infectivity factors and potential targets for development of new therapeutic strategies. Biochim Biophys Acta 2008;1780:362 - 69

Tanaka, AK, Valero, VB, Takahashi, HK, Straus, AH. Inhibition of *Leishmania (Leishmania) amazonensis* growth and infectivity by aureobasidin A. J Antimicrob Chemother 2008;59:487 - 92

Wu WI, Lin YP, Wang E, Merrill AH, Jr., Carman GM. Regulation of phosphatidate phosphatase activity from the yeast *Saccharomyces cerevisiae* by sphingoid bases. J Biol Chem 1993;268:13830 - 37

Zhang J-H, Chung TDY, Oldenburg KR. A simple statistical parameter for use in evalutation and validation of high throughput screening assays. J Biomol Screening 1999;4:67 - 73

Zhang K, Hsu F-F, Scott DA, Docampo R, Turk J, Beverley SM. *Leishmania* salvage and remodelling of host sphingolipids in amastigote survival and acidocalcisome biogenesis. Mol Microbiol 2005;55:1566 – 78

Zhang O, Wilson MC, Xu W, Hsu FF, Turk J, Kuhlmann FM, Wang Y, Soong L, Key P, Beverley SM, Zhang K. Degradation of host sphingomyelin is essential for *Leishmania* virulence. PLoS Pathog 2009;5:e1000692

Figure legends

Figure 1 Separation of NBD-C$_6$-IPC product from NBD-C$_6$-ceramide substrate by anion exchange chromatography

Thin layer chromatography analysis of fractions demonstrating the separation of NBD-C$_6$-IPC product from NBD-C$_6$-ceramide substrate.

1 Reaction product; 2 Column flow through; 3 - 5 Methanol wash; 6 - 9 Elution

Cer - NBD-C$_6$-ceramide; IPC - NBD-C$_6$-IPC

Figure 2 Turnover of *Lmj*IPCS in CHAPS-washed and crude (unwashed) microsomal preparations.

Measured by the incorporation of the fluorescent acceptor substrate, NBD-C$_6$-ceramide, into NBD-C$_6$-IPC product. Fluorescent IPC was quantified following fractionation by HPTLC as described.

A   Assay of *Lmj*IPCS activity in crude or washed microsomes with (black) or without (grey) the addition of the donor substrate, bovine phosphatidylinositol (PI). The background due to endogenous PI (grey) is reduced after washing the membraneous material. Results normalized with respect to +PI samples.

B   The specific activity of *Lmj*IPCS, as determined by the formation of IPC, is enhanced in the washed microsomes. Note 2-fold increase in specific activity (based on total protein content per assay).

Figure 3 *Lmj*IPCS turnover versus time, enzyme concentration and in presence of DAG

Determined using the 96-well plate formatted assay as described, with fluorescent NBD-C_6-ceramide as acceptor substrate (5 µM), and bovine phosphatidylinositol (PI; 100 µM) as the donor substrate. IPC quantified with respect to NBD-C_6-ceramide standard curve. All points in triplicate, error bars shown.

A *Lmj*IPCS turnover versus time. Turnover defined as pmol IPC produced per unit of enzyme (pmol.U^{-1}) under the conditions employed. R^2 = 0.95

B *Lmj*IPCS turnover versus DAG concentration. Turnover is defined as pmol IPC produced per minute (pmol.min^{-1}.U^{-1}) under the conditions employed. R^2 = 0.86

C *Lmj*IPCS turnover versus enzyme concentration: linear range. Turnover is defined as pmol IPC produced per minute (pmol.min^{-1}) under the conditions employed. R^2 = 0.98

Figure 4 *Lmj*IPCS turnover versus acceptor substrate (NBD-C$_6$-ceramide) and donor substrate (phosphatidylinositol) concentrations

Determined using the 96-well plate formatted assay as described, with fluorescent NBD-C$_6$-ceramide as acceptor substrate, and bovine phosphatidylinositol (PI) as the donor substrate. IPC quantified with respect to NBD-C$_6$-ceramide standard curve. All points in triplicate, error bars shown.

A   *Lmj*IPCS turnover (defined as pmol IPC.min^{-1}.U^{-1}; v_0) demonstrated apparent Michaelis-Menton kinetics - $v_o = V_{max} [S] / (K_m + [S])$ - with respect to the acceptor substrate NBD-C$_6$-ceramide (S). Non-linear analysis calculated the apparent K_m = 3.5±0.35 µM; and the apparent V_{max} = 2.1±0.1 pmol.min^{-1}.U^{-1}. R² = 0.97, indicating a good fit to the model. [PI] = 100 μM.

B   *Lmj*IPCS turnover (v_o) with respect to the donor substrate (S), phosphatidylinositol (PI), did not fit the Michaelis-Menten model. R² = 0.76. [NBD-C$_6$-ceramide] = 5 μM.

C   However, *Lmj*IPCS turnover (v_o) with respect to PI fits a Michaelis-Menten model at high NBD-C$_6$-ceramide concentration. R² = 0.93. Non-linear analysis calculated the apparent K_m = 22.8±4.6μM and the apparent V_{max} 2.0±0.07 pmol.min^{-1}.U^{-1}. [NBD-C$_6$-ceramide] = 20 μM.

Figure 5 *Lmj*IPCS turnover with varying acceptor substrate (NBD-C$_6$-ceramide) and different fixed donor substrate (phosphatidylinositol) concentrations

Determined using the 96-well plate formatted assay as described, with fluorescent NBD-C$_6$-ceramide as acceptor substrate, and bovine phosphatidylinositol (PI) as the donor substrate. IPC quantified with respect to NBD-C$_6$-ceramide standard curve. All points in triplicate, error bars shown as indicated. Donor (PI) and acceptor (ceramide) substrate concentrations varied as indicated.

A Plots of $1 / v_0$ vs. $1 / [S]$%, where S is NBD-C$_6$-ceramide as a molar fraction. Initial velocities (v_0) were determined with six concentrations of PI (12.5, 25, 37.5, 87.5 and 100 µM). The data points were generated from three independent determinations of v_0. Error bars were omitted for clarity.

B Plot of the intercepts of $1 / v_0$ from A against $1 / [S]$%, where S is PI as a molar fraction.

C Simulation and experimental data
[NBD-C$_6$-ceramide] = variable, [PI] = 100 μM.

D Simulation and experimental data
[NBD-C$_6$-ceramide] = 20 μM, [PI] = variable.

Figure 6 Competitive inhibition of *Lmj*IPCS activity

Determined using the 96-well plate formatted assay as described, with fluorescent NBD-C_6-ceramide as acceptor substrate, and bovine phosphatidylinositol (PI) as the donor substrate. IPC quantified with respect to NBD-C_6-ceramide standard curve. All points in triplicate, error bars shown. Donor substrate (PI) concentration at 100 µM, acceptor (NBD-C_6-ceramide) substrate at 5 µM.

$\log IC_{50} = \log(10^{\log Ki}(1+[\text{NBD-}C_6\text{-Cer}] / \text{NBD-}C_6\text{-Cer } K_m))$

$[\text{NBD-}C_6\text{-Cer}] = 5.0$ µM, $K_m = 3.5$ µM

A   *N*-acetylsphingosine is a competitive inhibitor of *Lmj*IPCS: $\log IC_{50} = 1.2 \pm 0.2$; $IC_{50} = 16$ µM; $R^2 = 0.83$

B   D-*erythro*-sphingosine is a competitive in*hibitor of Lmj*IPCS: $\log IC_{50} = 1.7 \pm 0.2$; $IC_{50} = 53$ µM; $R^2 = 0.93$

Figure 7 Mass spectrometric analyses of reaction products from *N*-acetyl-D-*erythro*-sphingosine

Negative ion mass spectrum demonstrating that *N*-acetyl-D-*erythro*-sphingosine (AcSph, mass = 340.3) is a substrate for *Lmj*IPCS, giving the product inositol phosphoryl acetyl-D-*erythro*-sphingosine (IP-AcSph, mass = 582.3).

Supplementary data

S1 Derivation of Equation 3

The hypothetical catalytic reaction scheme assuming double displacement kinetics and initial rate conditions.

E_D: *Lmj*IPCS associated with the detergent, CHAPS; **PI**: Phosphatidylinositol; $E_D.$**PI**: *Lmj*IPCS-PI complex; **DAG**: Diacylglycerol; $E_D.$**IP**: Phosphorylated intermediate *Lmj*IPCS with phosphorylinositol group; **Cer**: Ceramide; $E_D.$**IP.Cer**: *Lmj*IPCS-IP-Ceramide complex; $E_D.$**IPC**: *Lmj*IPCS-IPC complex; **IPC**: Inositol phosphorylceramide.

Table 1

	L. major promastigotes	*L. mexicana* promastigotes	*L. mexicana* amastigotes
Miltefosine			
logLD_{50}	0.20	0.15	1.10
SE logLD_{50}	0.06	0.06	0.03
LD_{50} μM	1.59	1.41	12.6
Sphingosine			
logLD_{50}	0.81	0.91	1.12
SE logLD_{50}	0.13	0.14	0.04
LD_{50} μM	6.49	8.18	13.3
Acetylceramide			
logLD_{50}	1.63	1.81	ND
SE logLD_{50}	0.14	0.18	ND
LD_{50} μM	43.0	64.5	ND

ND = not determined; LD_{50} = lethal dose, 50%; SE = standard error

Figure 1
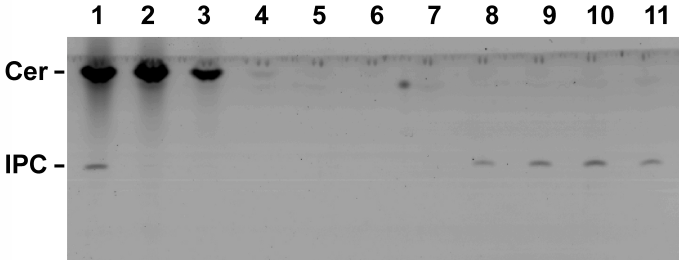
Figure 2
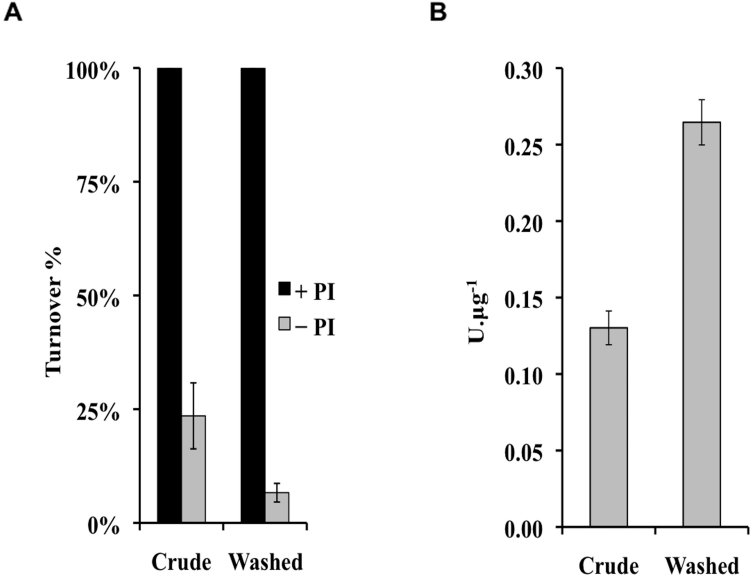
Figure 3

A
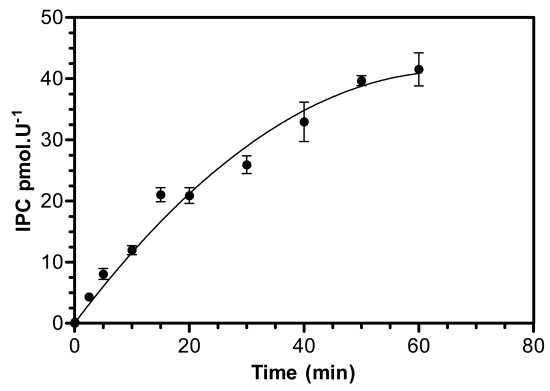
B
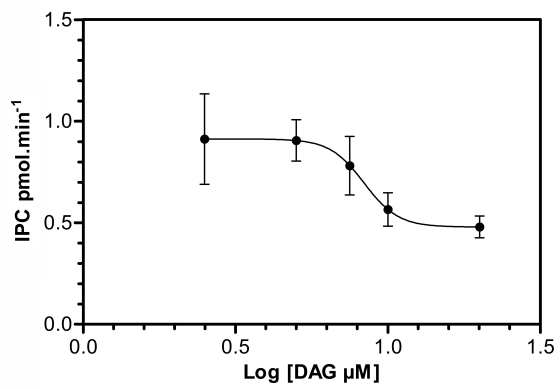
C
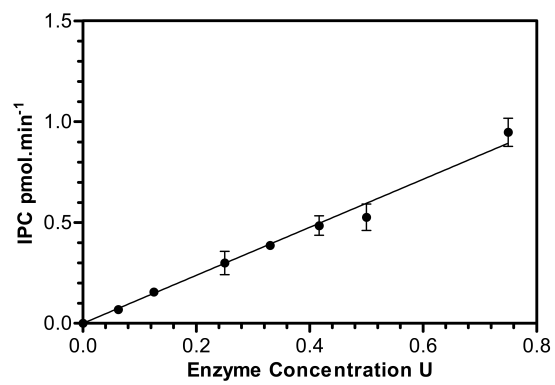
Figure 4

A
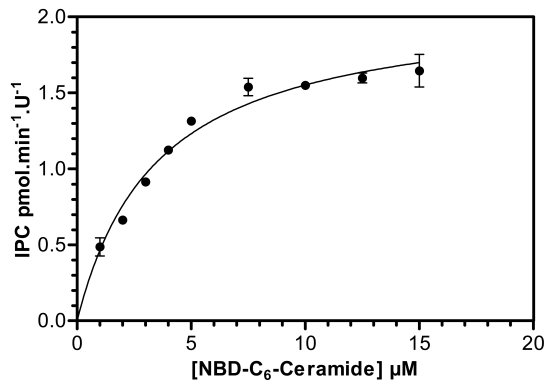
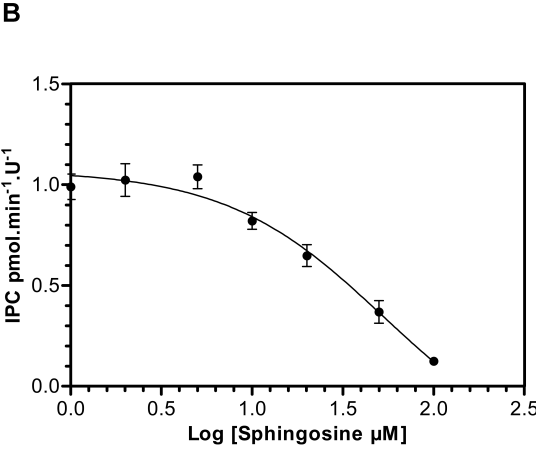**B**

C

Figure 5

Figure 6

A

B

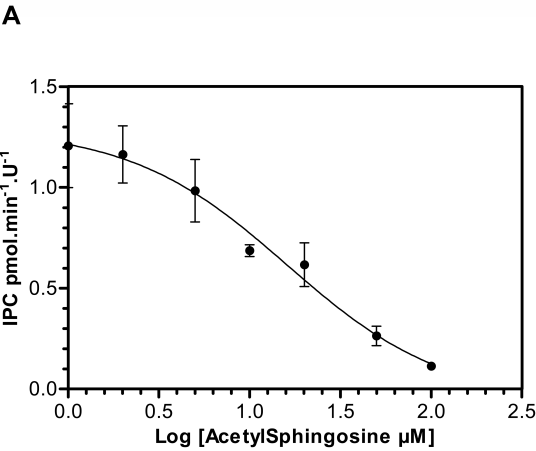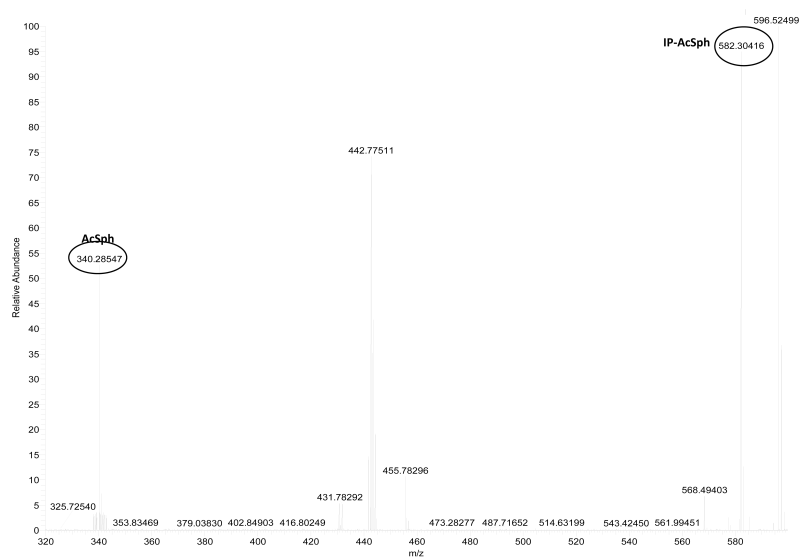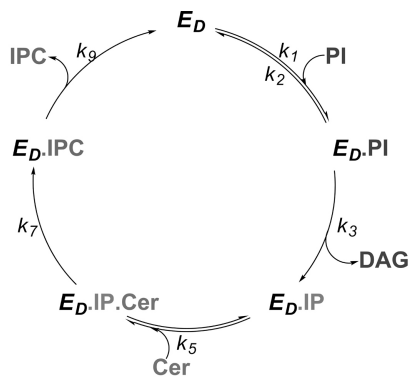**Figure 7**

S1
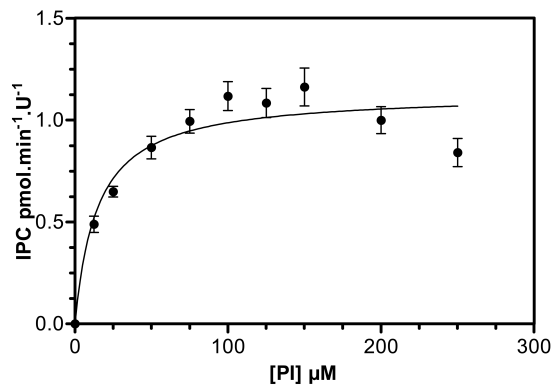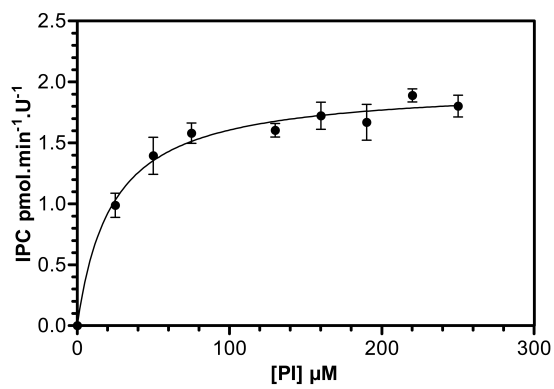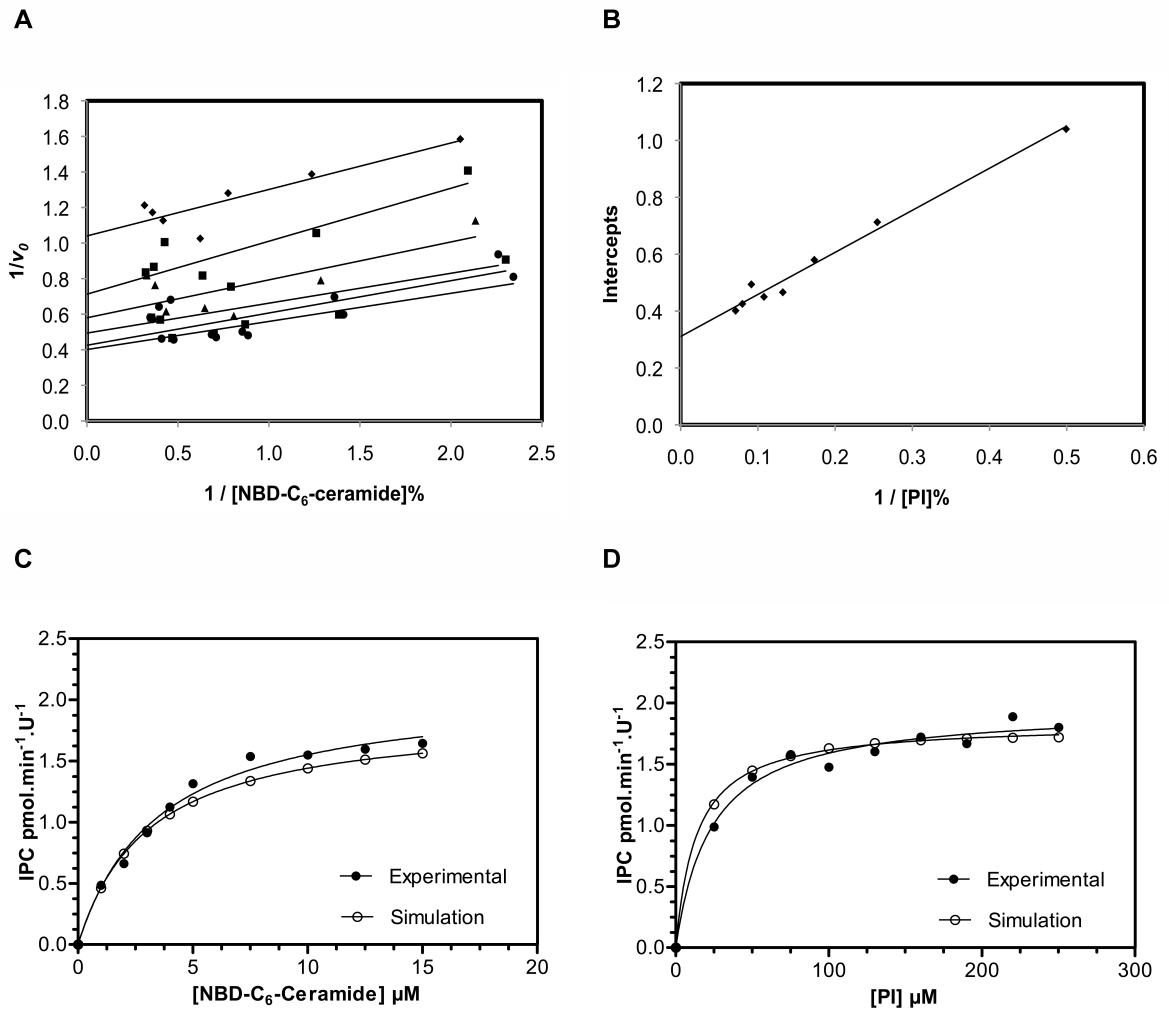
$$\frac{[E_T]}{v} = \varnothing_0 + \varnothing_A \frac{1}{[PI]} + \varnothing_B \frac{1}{[Cer]} \ where,$$

$$\varnothing_0 = \left(\frac{1}{k_9} + \frac{1}{k_7} + \frac{(k_6 + k_7)}{k_3 k_7} - \frac{k_6}{k_3 k_7} \right), \qquad \varnothing_A = \left(\frac{1}{k_1} + \frac{k_2(k_6 + k_7)}{k_1 k_3 k_7} - \frac{k_2 k_6}{k_1 k_3 k_7} \right)$$

$$\varnothing_B = \left(\frac{(k_6 + k_7)}{k_5 k_7} \right)$$